

Article

Investigation of Mechanical Properties for Basalt Fiber/Epoxy Resin Composites Modified with La

Chong Li ^{1,*}, Haoyu Wang ^{2,*}, Xiaolei Zhao ³, Yudong Fu ² , Xiaodong He ⁴ and Yiguo Song ¹

¹ Center for Engineering Training, Harbin Engineering University, Harbin 150001, China; songyiguo@hrbeu.edu.cn

² College of Materials Science and Chemical Engineering, Harbin Engineering University, Harbin 150001, China; fuyudong@hrbeu.edu.cn

³ China Offshore Oil Engineering Company, No. 199 Haibin 15 Road, TianjinPort Free Trade Zone, Tianjin 300461, China; zhaoxiaol@cooec.com.cn

⁴ National Key Laboratory of Science and Technology on Advanced Composites in Special Environment, Harbin Institute of Technology, Harbin 150001, China; hexd@hit.edu.cn

* Correspondence: lichong@hrbeu.edu.cn (C.L.); haoyuwang@hrbeu.edu.cn (H.W.)

Abstract: As an efficient reinforcing material in resin matrix composites, the application of basalt fibers (BFs) in composites is limited by the poor interfacial adhesion between BFs and the resin matrix. In this study, to obtain the basalt fibers/epoxy resin composites with enhanced mechanical properties, the modification solution containing different concentrations of Lanthanum ions (La³⁺) was synthesized to modify the BFs surfaces to enhance the poor interfacial adhesion between BFs and the matrix. The morphology, the chemical structure and the chemical composition of the modified BFs surface were observed and detected by scanning electron microscopy, Fourier transform infrared spectroscopy and X-ray photoelectron spectroscopy, respectively. The results show that, after BFs were soaked in the modification solution, the more active groups (C=O, –OH, C–O, etc.) were introduced to the BFs surfaces and effectively enhanced the bond strength between BFs and the resin matrix. The obtained mechanical performances of prepared basalt fibers/epoxy resin composites showed that the tensile strength, bending strength and interlaminar shear strength (ILSS) were improved with the modified BFs, and reached to 458.7, 556.7 and 16.77 Mpa with the 0.5 wt.% La. Finally, the enhancement mechanism of the modification solution containing La element is analyzed.

Keywords: basalt fibers; composites; mechanical properties; surface engineering



Citation: Li, C.; Wang, H.; Zhao, X.; Fu, Y.; He, X.; Song, Y. Investigation of Mechanical Properties for Basalt Fiber/Epoxy Resin Composites Modified with La. *Coatings* **2021**, *11*, 666. <https://doi.org/10.3390/coatings11060666>

Academic Editor: Maude Jimenez

Received: 22 April 2021

Accepted: 29 May 2021

Published: 31 May 2021

Publisher's Note: MDPI stays neutral with regard to jurisdictional claims in published maps and institutional affiliations.



Copyright: © 2021 by the authors. Licensee MDPI, Basel, Switzerland. This article is an open access article distributed under the terms and conditions of the Creative Commons Attribution (CC BY) license (<https://creativecommons.org/licenses/by/4.0/>).

1. Introduction

In the past years, many studies have been conducted on the applicability of basalt fibers (BFs). As a reinforcing material for composites, BFs (mainly composed by SiO₂) can be prepared from basalt rocks using conventional equipment with the advantage on the low-cost process of melting and drawing [1]. Compared with other fiber materials, BFs have the excellent properties such as high tensile strength, high E-modulus, high abrasion strength, high temperature resistance, high resistance to aggressive media, excellent thermal and sound insulation, good chemical stability [2]. Moreover, the mechanical properties of BFs can be kept without significant decrease in the operating temperature range of 200–600 °C [3]. In addition, the environmentally friendly preparation and recycling process of BFs significantly improves its demand for the modern market [1,4–6]. Thus, the BFs might be a promising reinforced material as the candidate of glass and carbon fibers in composite materials, and have been attractive in the application of friction materials, corrosion resistance materials, heat shields, thermal insulating barriers and hot fluid transportation pipes in many fields [7].

Especially in the field of flywheel rotors' structural materials, the fiber-reinforced resin matrix composite flywheel was generally to replace the traditional metal flywheel due to

their high strength, high energy storage density and low specific volume [8]. Compared with the common reinforced fibers (glass and carbon fibers), the BFs represent an alternative as the substitution due to their excellent properties.

However, the smooth and chemically inert surface of BFs [9–11] results in the low interfacial adhesion between BFs and matrix (here below referred as interfacial adhesion) to reduce the composite materials' performance. To enhance the interfacial adhesion, many studies have been conducted to modify the fiber surface, such as the plasma modification technology, the oxidized modification technology, the coating modification technology, and so on [12–23]. Manikandan and Jain et al. [3,24] increased the surface roughness of BFs by the acid and alkali chemical treatments, which improved interfacial bonding strength between fibers and matrix. Kim et al. [11] and Ricciardi [25] used surface treatment of BFs by low-temperature atmospheric oxygen plasma and SF₆ plasma to increase the wettability of BFs remarkably, and improve adhesive force between fiber/resin interfaces accompanied by physical etching and by the formation of chemical functional groups containing oxygen and nitrogen on the fiber surface. This increased the interlaminar fracture toughness of basalt/epoxy woven composites. Wei et al. proposed the coating modification as an effective way in improving the mechanical properties of BFs and the properties of basalt fiber/epoxy resin composites [1,6]. Cheng et al. [26–28] investigated the effects of surface-treated F-12 aramid fibers and carbon fibers on the interfacial adhesion between fibers and matrix. They found that rare earth modification solution treatment can increase the concentration of reactive functional groups on fiber surface through chemical coordinating reaction. Additionally, the interfacial adhesion was promoted obviously and the tensile properties of composites improved significantly. Meanwhile, the tensile strengths of single fibers are almost not affected by rare earth modification solution treatment. It exhibits an attractive method to treat BFs with the rare earth modification solution due to its high efficiency, simple process, environmentally friendly characteristics, and preservation of fiber tensile strengths. Thus, with the few studies on BFs modified by rare earth elements, the modification study on BFs to prepare fiber-reinforced composites with excellent performance was promising.

In this study, the rare earth modification solution was synthesized by adding different concentrations of element La. The effects of the BFs surfaces with different concentration of element La were investigated. The mechanical properties of the composite materials, such as the tensile strength, the bending strength and the interlaminar shear strength (ILSS) were detected. The modification mechanism of the BFs surface was also discussed.

2. Experimental Details

2.1. Materials

The used BFs cloth (223 g/km, unidirectional cloth) with an average fiber of diameter (5.9 μm) was manufactured by Shanxi Basalt Fiber Technology Co., Ltd., Taiyuan, China. The elastic modulus and the tensile strength of the BFs cloth were about 7.5 and 1835 MPa, respectively. The epoxy resin (LY564) and the curing agent (22964, aliphatic polyamine curing agent) were from Huntsman Co., Ltd. (The Woodlands, TX, USA). The following chemical reagents were used: acetone and nitric acid (analytical reagent, provided by Tianjin Tianda Chemical Reagent Factory, Tianjin, China), absolute ethyl alcohol (analytical reagent, produced by Tianjin Tianli Chemical Reagent Co., Ltd., Tianjin, China), citric acid and urea (analytical reagent, provided by Tianjin Zhiyuan Chemical Reagent Co., Ltd., Tianjin, China), lanthanum chloride (99.99%, manufactured by Jining Zhongkai New Type Material Co., Ltd., Jining, China).

2.2. Treatment of Fibers

The BFs cloth was cut into 260 × 35 mm². After immersed in acetone for 48 h at room temperature to remove the protective coating on the surface of BFs, the fibers were dried in a drying oven at 100 °C for 1 h. The dried fiber cloth was soaked in the concentrated nitric acid with constant temperature water bath at 60 °C for 2 h to improve the roughness and

the –OH numbers of the fibers' surfaces [29]. Washing the fibers 3–4 times with distilled water to remove acid fluid from their surfaces, the PH value on the surface of the fibers was adjusted to 7. Finally, the fibers were dried in a drying oven at 100 °C for 1 h and conserved in the dryer.

According to a certain weight ratio, the composition of the BFs modification solution were uniformly mixed at room temperature, as shown in Table 1. Additionally, five kinds of rare earth modification solution were prepared with different La³⁺ concentrations of 0.1, 0.3, 0.5, 0.7, and 0.9 wt.% After immersed in the rare earth modification solution for 2 h, the treated BFs were dried in the drying oven at 100 °C for 1 h.

Table 1. Composition of the BFs modification solution.

Name	Molecular Formula
Ethyl alcohol	C ₂ H ₆ O
Citric acid	C ₆ H ₈ O ₇
Urea	CO(NH ₂) ₂
Nitric acid	HNO ₃
Lanthanum chloride	LaCl ₃ ·7H ₂ O

2.3. Fabrication and Measurements of Basalt Fiber/Epoxy Resin Composites

The prepared BFs was immersed in epoxy resin/curing agent mixture at volume ratio 4:1. With the hand lay-up method, the BF/ERCs were paved as three layers in the mold, and fabricated after curing in a drying oven at 120 °C for 15 min and 140 °C for 2 h, respectively.

The change of BFs' chemical structure was determined in the transmission mode using Fourier transform infrared spectroscopy (FT-IR, Perkin Elmer 100, Waltham, MA, USA). X-ray photoelectron spectroscopy (XPS) using a PHI 5700 ESCA System equipped with an Al-Ka X-ray source (New York, NY, USA), analyzed the chemical composition of the BFs surfaces. The surface morphologies of BFs and the fracture surface morphologies of the composites were examined using scanning electron microscopy (SEM, JSM-6480, Tokyo, Japan).

The tensile test and the bending test were carried out to determine the tensile strength and the bending strength of BF/ERCs, respectively. The ILSS of BF/ERCs was measured by the three-point short-beam bending test. Due to the details of the mechanical tests shown in Table 2 below, the specimens were cut according to the following dimensional requirement.

Table 2. Details of the mechanical tests.

Test	Standard Test Method	Equipment	Loading Speed mm/min	Thickness (mm)	Width (mm)	Span (mm)
Tensile	GB/T1447-2005	Universal testing machine	5.0	1.5–3	25	100 ± 0.5
Flexural	GB/T1449-2005	(UTM, WOW-50, Jinan Liangong Testing Technology Co., Ltd., Jinan, China)	constant	1.5–3	15 ± 0.5	22.5
Shear	GB3357-82		2.0	2.5	10	12.5

3. Results

3.1. FT-IR Spectra of BFs

The chemical structures of untreated and treated BFs were obtained with FT-IR spectroscopy, as shown in Figure 1. The characteristic peaks of –OH at 3450 cm^{−1} and C=O at 1630 cm^{−1} were observed in the untreated BFs. In addition, the peaks of –CH₂ appeared at 2921 and 2844 cm^{−1}, respectively. As the main composition of BFs, the peak of Si-O from SiO₂ of BFs appeared at 860 cm^{−1}.

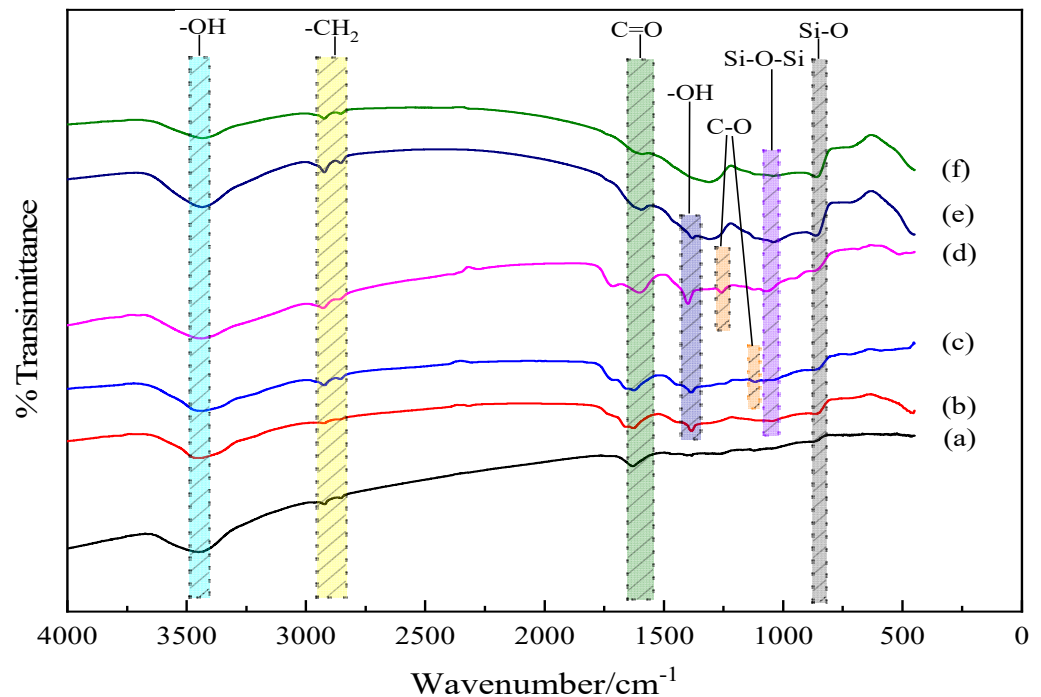


Figure 1. FT-IR spectra of BFs: (a) untreated; (b) treated with modification solution containing La^{3+} 0.1 wt.%; (c) treated with modification solution containing La^{3+} 0.3 wt.%; (d) treated with modification solution containing La^{3+} 0.5 wt.%; (e) treated with modification solution containing La^{3+} 0.7 wt.%; (f) treated with modification solution containing La^{3+} 0.9 wt.%.

For BFs treated with the 0.1 wt.% La^{3+} rare earth modification solution, the new absorption peaks of C=O at 1660 cm^{-1} and -OH at 1384 cm^{-1} appeared in the range of $4000\text{--}1330\text{ cm}^{-1}$, and the peaks of -CH₂ at 2917 and 2845 cm^{-1} from the citric acid were broader than those of the untreated BFs, indicating that the La^{3+} was successfully absorbed on the BFs' surface with the introduced -CH₂- from the acyl group and citric acid, which also brought C=O. The absorption band at the peak of 1046 cm^{-1} referred to the formation of along with the peak of shifting from 860 to 863 cm^{-1} , stating that the Si-OH from the hydrolysis of SiO₂ react with itself or the introduced -COOH under dehydration condensation reaction to produce Si-O-Si and more Si-O. With La^{3+} concentration increasing to 0.3 wt.% in the rare earth modification solution, the new peak of C-O from the citric acid along with the introduced La^{3+} at 1116 cm^{-1} appeared in the FT-IR spectrum. Moreover, the peaks of -CH₂ at 2922 and 2859 cm^{-1} exhibited obviously. It indicated that the La^{3+} was absorbed to the surface with -COOH and -CH₂ from citric acid. When La^{3+} concentration was up to 0.5 wt.%, the vibration frequency of C-O increased from 1116 to 1260 cm^{-1} , and that of C=O stretched from 1668 to 1716 cm^{-1} , accompanied by the urea in the modification solution. Due to the strong affinity of La^{3+} to nonmetal element, the La^{3+} could combine with urea and citric acid under the coordination reaction to introduce the C=O and C-O from the modification solution, resulting that more active oxygen-contained functional groups were introduced onto the fiber surfaces with the increasing La^{3+} concentration.

With the La^{3+} concentration above 0.5 wt.%, the peak of C=O began to disappear. At the La^{3+} concentration of 0.9 wt.%, the peak disappearances of C-O at 1260 cm^{-1} and the other weakened characteristic peaks were observed, implying that superabundant active groups introduced by the excess La^{3+} were aggregated on the BFs to be supersaturated and further destroyed formed macromolecular membrane on the BFs' surface to trigger the loss of active groups.

3.2. XPS Results of BFs

3.2.1. XPS Results of BFs

As shown in Figure 2 and Table 3, the XPS survey spectra and the detected atomic concentration of the elements C, O, N and Si on the BFs surfaces were respectively obtained to analyze the chemical composition of the BFs surface. On the surfaces of BFs treated with the rare earth modification solution, the concentration of element C decreased and then increased with the increase of La^{3+} concentration, but the changes of the elements O and N were contrary. The proportions of O/C and N/C on the BFs surfaces had the same variation trend with the concentration of element C. When La^{3+} concentration was 0.5 wt.%, the proportions of O/C and N/C reached maximum values, confirming that the BFs surfaces contained the largest number of active oxygen-containing groups.

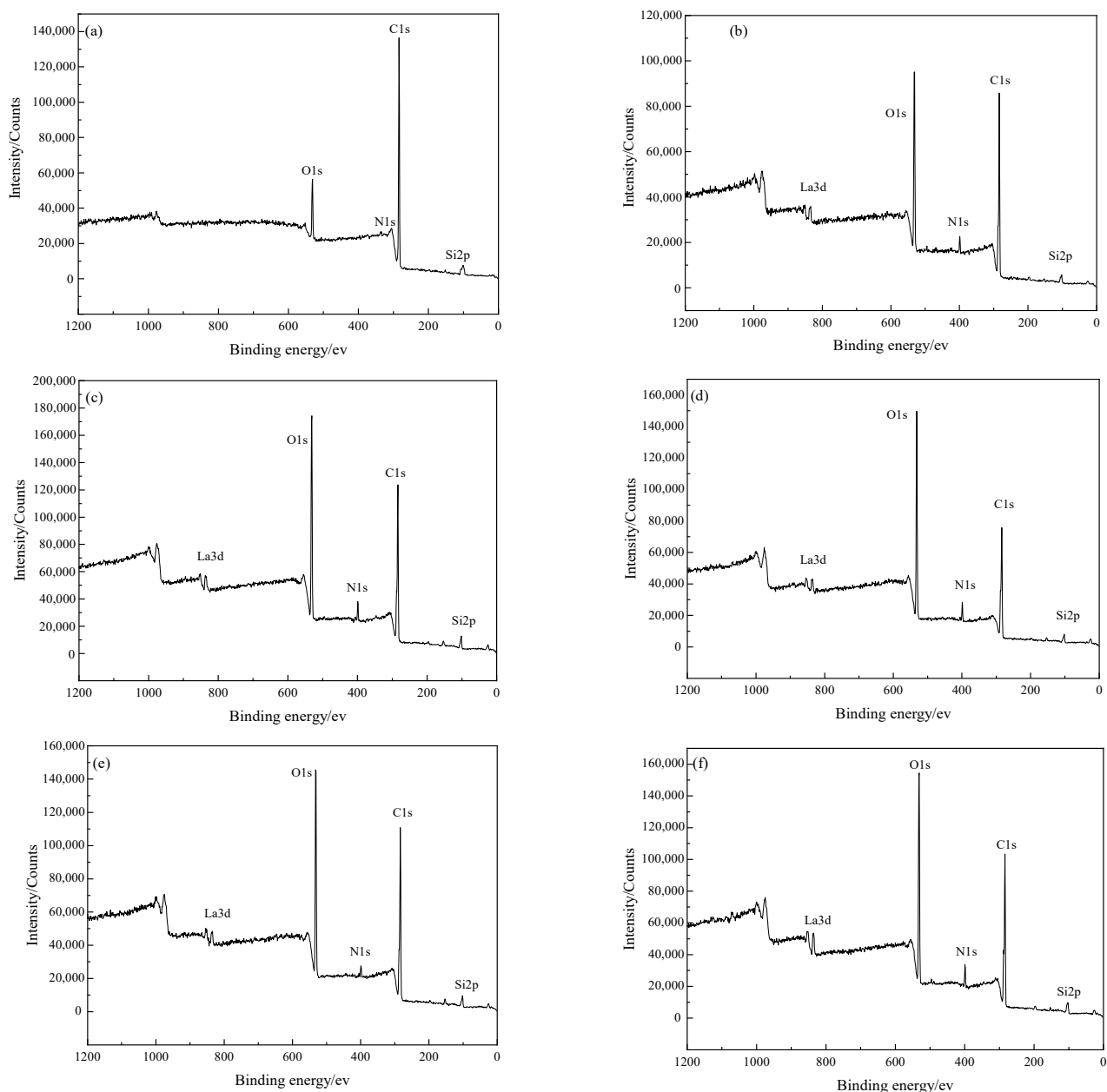


Figure 2. XPS survey spectra of BFs: (a) untreated; (b) treated with modification solution containing La^{3+} 0.1 wt.%; (c) treated with modification solution containing La^{3+} 0.3 wt.%; (d) treated with modification solution containing La^{3+} 0.5 wt.%; (e) treated with modification solution containing La^{3+} 0.7 wt.%; (f) treated with modification solution containing La^{3+} 0.9 wt.%.

Table 3. XPS results of BFs.

Specimens	Elements (%)					O/C	N/C
	C	O	Si	N	La		
Untreated	80.65	15.06	2.47	0.78	-	0.19	0.01
0.1 wt.% La ³⁺	65.29	25.55	5.38	3.72	0.07	0.39	0.06
0.3 wt.% La ³⁺	56.14	28.62	5.59	7.63	0.22	0.51	0.14
0.5 wt.% La ³⁺	40.95	43.38	5.78	9.01	0.88	1.05	0.22
0.7 wt.% La ³⁺	50.42	33.97	6.31	8.36	0.94	0.67	0.17
0.9 wt.% La ³⁺	53.38	28.68	8.15	8.32	1.47	0.54	0.16

3.2.2. XPS Results of La on BFs Surfaces

The fitted curves of La3d spectra on BFs surface treated with different modification solution containing La³⁺ are presented in Figure 3. The spectra peaks of La3d in the treated BFs with the different La³⁺ modification solution concentrations (0.1, 0.3, 0.5, 0.7, and 0.9 wt.%) were corresponding to the bonding energies of 851.02, 851.77, 851.9, 852, and 852.1 eV, respectively. All the bonding energies were lower than that (853.0 eV) of the La corresponding to La3d in LaCl₃, indicating that the coordination chemical reactions occurred between the La and the O, C, N element of the treated fibers' surfaces to generate lanthanum coordination compounds on fibers' surfaces.

3.2.3. XPS Characterization of Element C on BFs Surfaces

The fitted curves of C 1s spectra and the detected functional groups contents on the BFs surfaces are presented in Figure 4 and Table 4, respectively. Three small peaks of C–C, C–O– and C=O appeared under the C 1s peak of the untreated BFs surfaces in Figure 4a, indicating that C atoms were combined with O atoms. The percentage of C atoms in the corresponding chemical state was represented with the area ratio of every small peak to the C 1s peak. Due to the low content of element N on BFs surfaces, the C–N bond could be ignored.

As seen in Figure 4b, with the peak appearance of –COOH in the fitted curves of C 1s spectra of the BFs, new functional groups were generated on the surface of BFs treated with the rare earth modification solution, besides the original ones. According to the low-to-high order of binding energy, these functional groups can be arranged as alcoholic hydroxyl (C–OH) or ether bond (C–O–C), carbonyl (C=O) and carboxyl (COOH). The C–C content on the BFs surfaces firstly decreased and then increased with La³⁺ concentration increasing, but the changes of the carbon–oxygen bond were contrary. When La³⁺ concentration was 0.5 wt.%, with the sum of C–OH/–C–O–C–, C=O and –COOH reaching to a maximum value (72.87%), the number of oxygen-containing groups on the BFs surfaces were the largest. As La³⁺ concentration exceeded 0.5 wt.%, the content of carbon–oxygen bond decreased. That was attributed to the fact that the abundant oxygen-containing groups introduced by excess La were aggregated on the fibers' surfaces and could not be stably absorbed to the fibers' surfaces with the weak Van der Waals force between La³⁺. Moreover, the aggregated supersaturated active oxygen-containing groups could also trigger the break of the origin formed macromolecular membrane on the fibers' surfaces, which led to the loss of active groups.

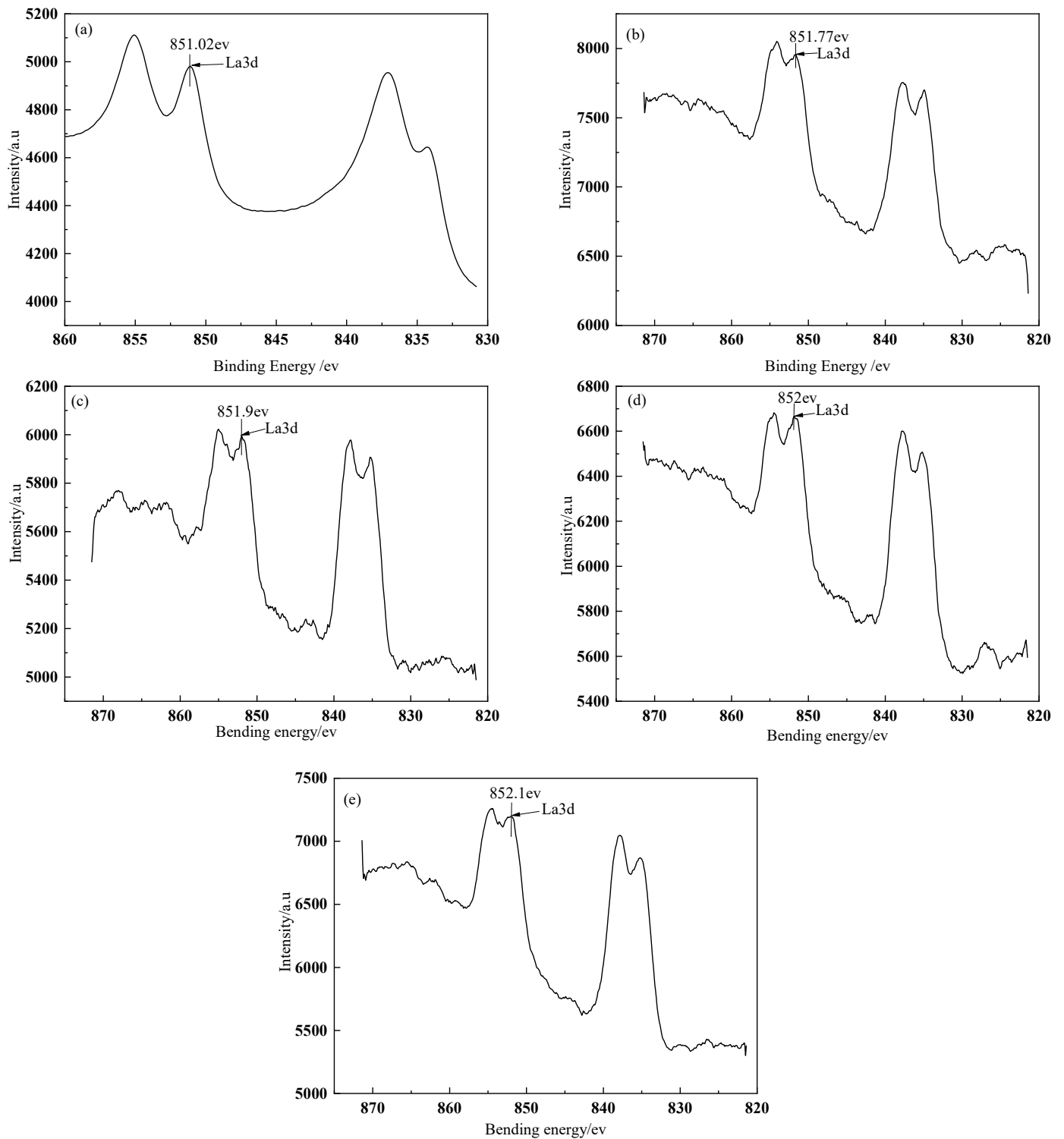


Figure 3. XPS survey spectra of La on BF surfaces: (a) treated with modification solution containing La³⁺ 0.1 wt.%; (b) treated with modification solution containing La³⁺ 0.3 wt.%; (c) treated with modification solution containing La³⁺ 0.5 wt.%; (d) treated with modification solution containing La³⁺ 0.7 wt.%; (e) treated with modification solution containing La³⁺ 0.9 wt.%.

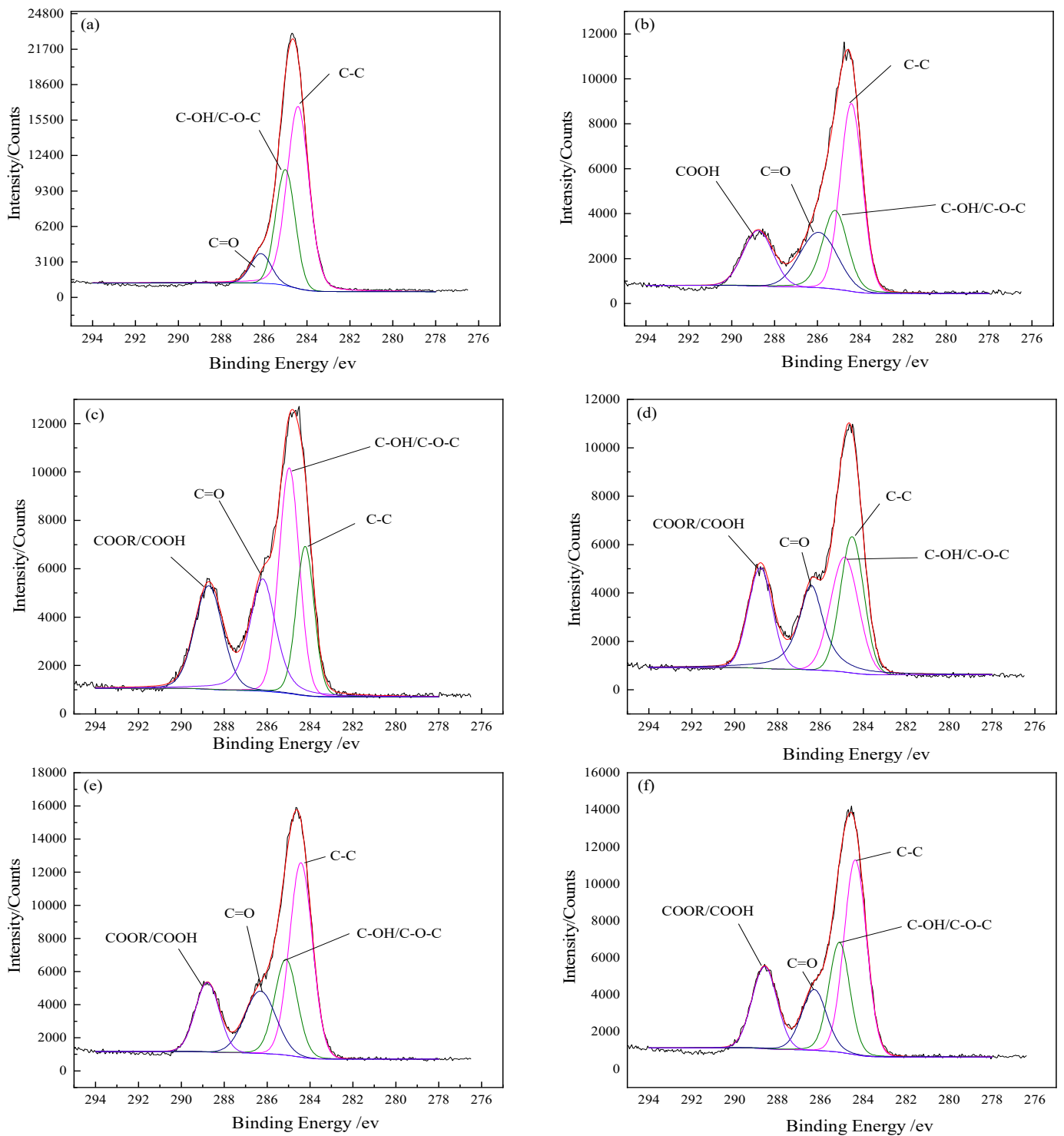


Figure 4. Fitted curves of C1s spectra: (a) untreated; (b) treated with modification solution containing La³⁺ 0.1 wt.%; (c) treated with modification solution containing La³⁺ 0.3 wt.%; (d) treated with modification solution containing La³⁺ 0.5 wt.%; (e) treated with modification solution containing La³⁺ 0.7 wt.%; (f) treated with modification solution containing La³⁺ 0.9 wt.%.

Table 4. C 1s results of BFs surfaces.

BFs	-C-C		C-OH/-C-O-C-		C=O		-COOH	
	Area Ratio (%)	Binding Energy (ev)						
Untreated	60.49	284.41	31.12	285	8.40	286.15	-	-
0.1 wt.% La ³⁺	41.89	284.33	21.23	285.15	20.56	286.473	16.32	288.89
0.3 wt.% La ³⁺	30.41	284.23	30.98	284.88	23.37	286.1	15.23	288.66
0.5 wt.% La ³⁺	27.13	284.52	27.36	284.87	24.56	286.43	20.96	288.8
0.7 wt.% La ³⁺	39.23	284.45	22.76	285.3	17.80	286.44	20.21	288.7
0.9 wt.% La ³⁺	42.18	284.37	22.98	285.11	15.35	286.29	19.49	288.6

3.2.4. XPS Characterization of Si Element on BFs Surfaces

The functional group contents on the BFs surfaces are presented in Table 5, according to the fitted curves of Si 2p spectra in Figure 5. Figure 5a showed that SiO₂ and Si-O-Si bonds appeared on the untreated BFs surfaces, affirming that SiO₂ was the main chemical composition of BFs surfaces. The existence of Si-O-Si bonds was ascribed to the formation of BFs connected by [SiO₄] tetrahedron, which could further form [Si₂O₇] under interaction and even the chain structure with a higher degree of polymerization. Under the hydrolysis of SiO₂ in the modification solution, the new functional group (Si-OH) was generated on the surface of BFs treated with the rare earth modification solution along with the obvious decrease of SiO₂. However, the increase of Si-O-Si was mainly ascribed to the dehydration condensation reaction of Si-OH bonds by themselves or active organic groups in the modification solution, such as -COOH and -OH.

Table 5. Si 2p results of BFs surfaces.

BFs	SiO ₂		Si-O-Si		Si-OH	
	Area Ratio (%)	Binding Energy (ev)	Area Ratio (%)	Binding Energy (ev)	Area Ratio (%)	Binding Energy (ev)
Untreated	71.14	102.59	28.86	101.75	-	-
0.1 wt.% La ³⁺	47.41	106.16	33.64	103.48	18.94	102.43
0.3 wt.% La ³⁺	40.15	105.85	36.81	103.37	23.04	102.47
0.5 wt.% La ³⁺	36.12	105.81	39.72	103.28	24.17	102.33
0.7 wt.% La ³⁺	51.80	105.97	27.32	103.25	20.88	102.18
0.9 wt.% La ³⁺	58.13	105.71	23.89	103.17	17.98	102.28

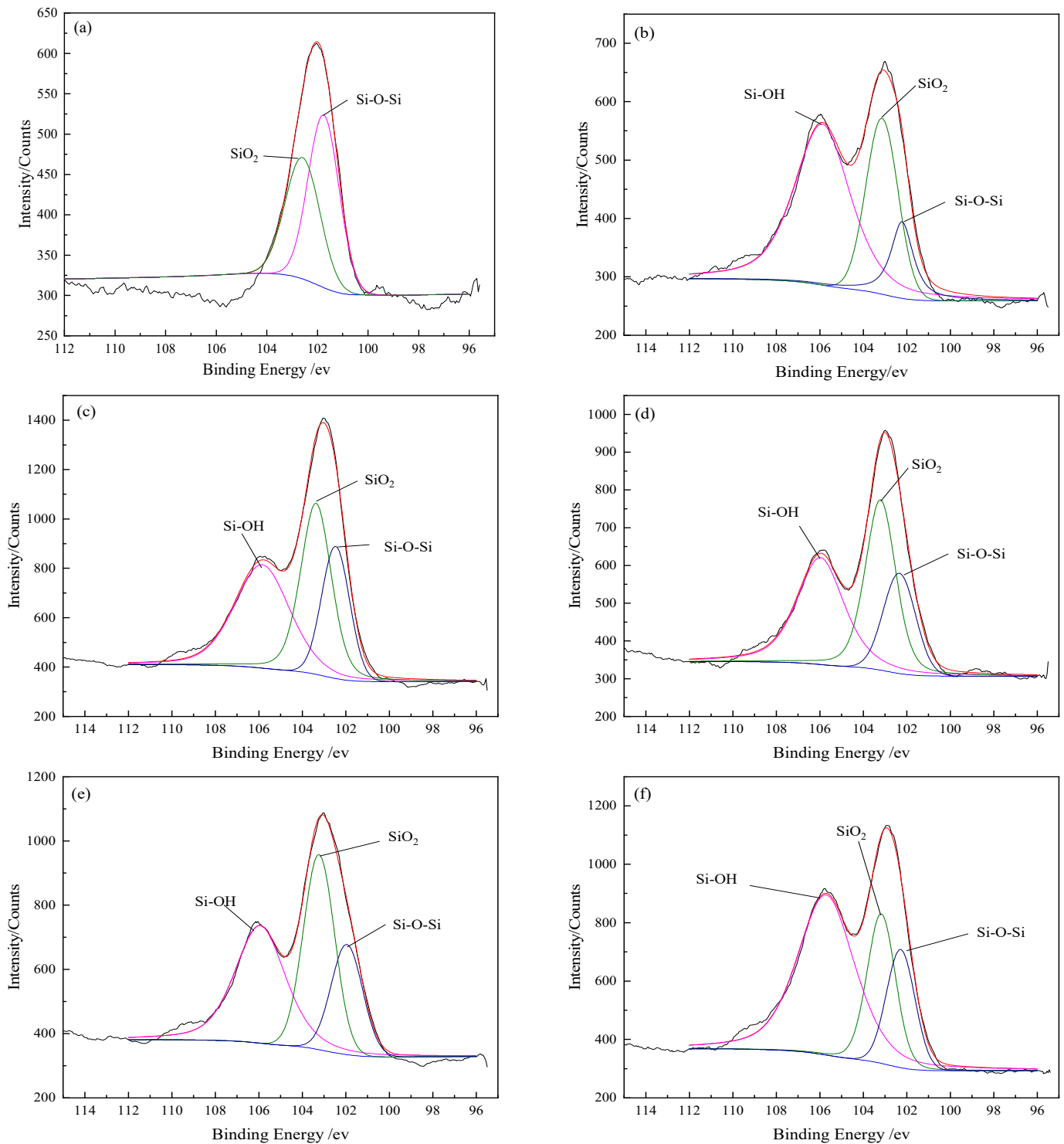


Figure 5. Fitted curves of Si element spectra: (a) untreated; (b) treated with modification solution containing La³⁺ 0.1 wt.%; (c) treated with modification solution containing La³⁺ 0.3 wt.%; (d) treated with modification solution containing La³⁺ 0.5 wt.%; (e) treated with modification solution containing La³⁺ 0.7 wt.%; (f) treated with modification solution containing La³⁺ 0.9 wt.%.

It can be seen that the SiO_2 content on the BFs surfaces firstly decreased and then increased with La^{3+} concentration increasing, but the content changes of Si–O–Si and Si–OH were contrary. When La^{3+} concentration was 0.5 wt.%, the SiO_2 content reached a minimum value (36.12%) corresponding to the highest contents of Si–O–Si and Si–OH. With the La^{3+} concentration beyond 0.5 wt.%, the ether bond was generated with the reaction of Si–OH and active groups in the rare earth modification solution. Accordingly, the hydrolysis of SiO_2 was compressed and the content of SiO_2 increased.

3.3. Basalt Fiber Surface Morphology

Figure 6 reveals the changes of BFs surface morphology after modification. The surfaces of untreated BFs were smooth without obvious grooves or salients in Figure 6a. Some particles formed through the process of the active groups drawn onto the fiber surfaces by the rare earth element, were attached to the surfaces of BFs treated with the rare earth modification solution containing La^{3+} concentration 0.1 wt.% in Figure 6b. Figure 6c,d shows that a trend of increasing particles was accompanied by an increasing concentration of La^{3+} . When La^{3+} concentration was up to 0.5 wt.%, a great number of small particles uniformly covered the fiber surfaces to form the fibers' coatings.

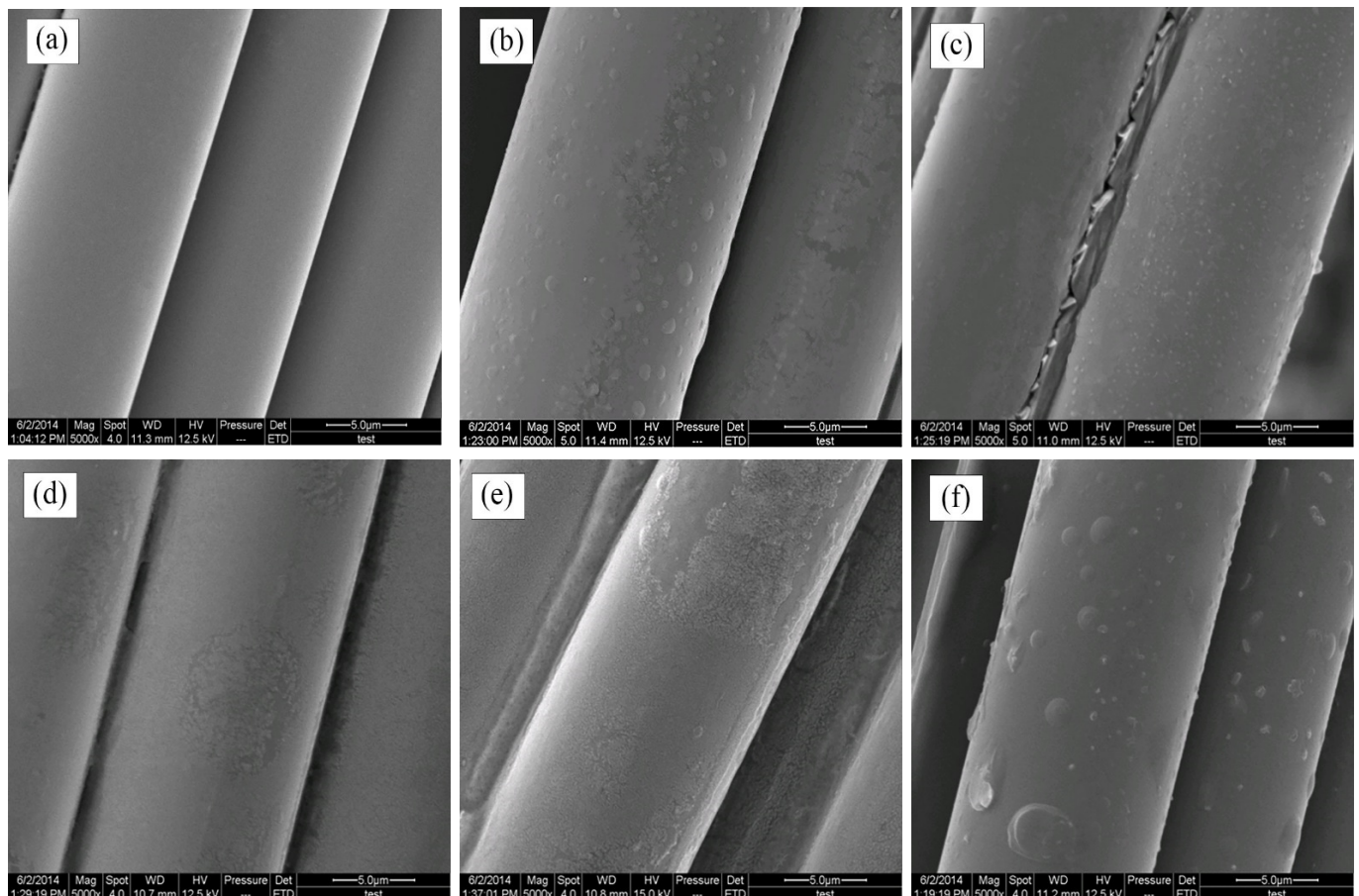


Figure 6. SEM images of BFs: (a) untreated; (b) treated with modification solution containing La^{3+} 0.1 wt.%; (c) treated with modification solution containing La^{3+} 0.3 wt.%; (d) treated with modification solution containing La^{3+} 0.5 wt.%; (e) treated with modification solution containing La^{3+} 0.7 wt.%; (f) treated with modification solution containing La^{3+} 0.9 wt.%.

As shown in Figure 6e,f, the particles decreased on the fiber surfaces, as La^{3+} concentration increased to 0.7 wt.%. When La^{3+} concentration was up to 0.9 wt.%, the excess rare earth elements were attached onto the fiber surfaces with the saturation of active groups,

resulting that only a few particles of inhomogeneous size were on the fibers. Moreover, these active groups were easy to bulge and even be broken under the function of tension.

3.4. Mechanical Properties of Basalt Fibers/Epoxy Resin Composites

Tensile, bending and ILSS standard tests were performed to analyze mechanical behavior of BF/ERCs. According to the obtained experimental data shown in Figures 7–9, the mechanical properties, including the tensile strength, the bending strength and ILSS of BF/ERCs, were improved by BFs treated with La^{3+} concentration increasing from 0.1 to 0.5 wt.%. The active functional groups attached to the fibers' surfaces, such as C=O and O–H, improved the fiber surface roughness and activity, and thus enhanced the adhesion between fibers and the composite matrix. The maximum values of the tensile strength, the bending strength and ILSS were up to 458.7, 556.7 and 16.77 Mpa, and increased by 56.22%, 103.32% and 88% compared with those of the unmodified ones, respectively.

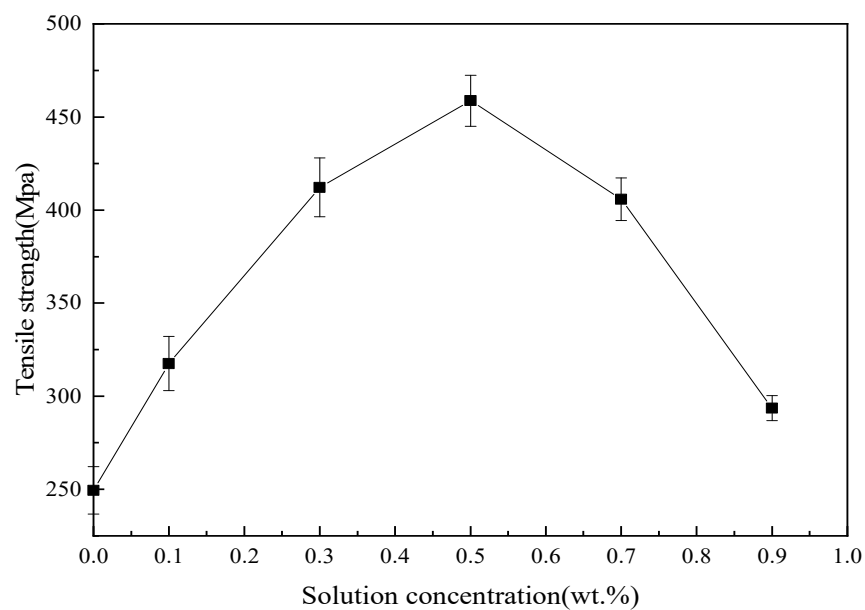


Figure 7. Tensile strength of BF/ERCs.

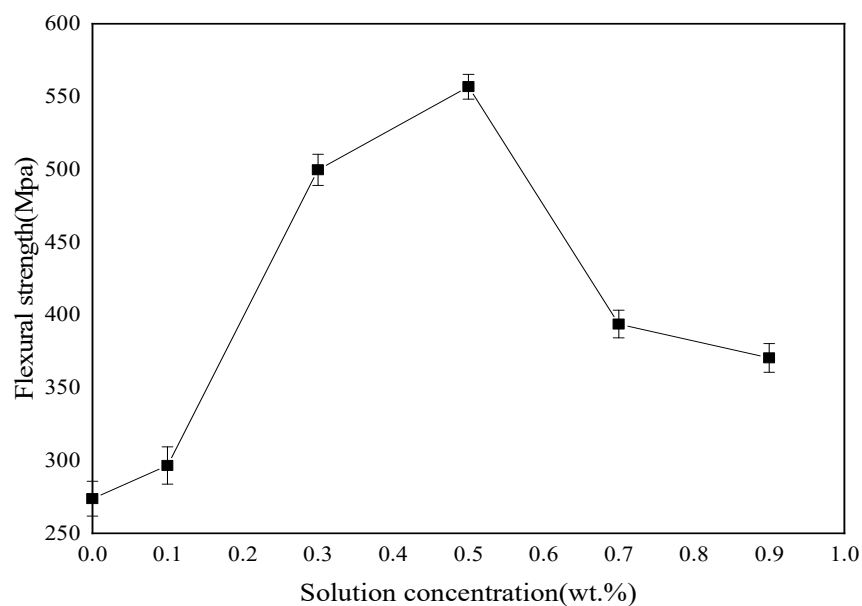


Figure 8. Flexural strength of BF/ERCs.

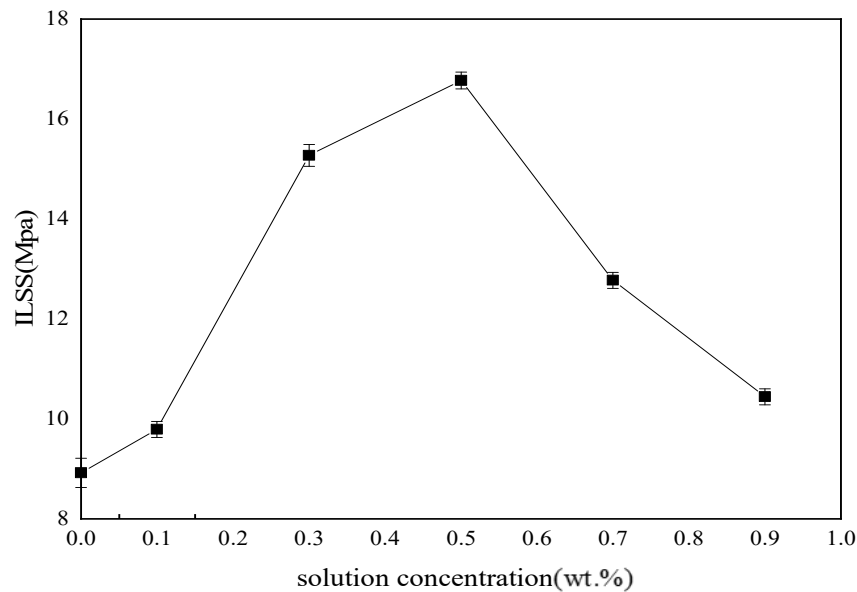


Figure 9. ILSS of BF/ERCs.

When La^{3+} concentration exceeded 0.5 wt.%, the mechanical strength of composites decreased as La^{3+} concentration increased. This may be ascribed to the fact that the excess active groups introduced by La^{3+} were aggregated to be supersaturated, and the triggered break of saturated active groups happened, leading to the loss of active groups. Moreover, the bits of grains on the interface of composite formed by the introduction of the excess La^{3+} to the fibers' surface also reduced the interface bonding strength.

3.5. Fracture Surfaces Morphology of Basalt Fibers/Epoxy Resin Composites

The fracture surfaces of untreated and treated BF/ERCs in the tensile test was observed by SEM. In Figure 10a, smooth fibers and grooves can be seen on the fracture surfaces of untreated composites. Caused by the worse interfacial adhesion between fibers and the resin matrix, the fibers can be easily separated or pulled out from the resin matrix, exhibiting the low tensile strength of composites.

There were a few resins on the fiber surfaces of composites treated with the rare earth modification solution containing La^{3+} concentration 0.1 wt.%, as shown in Figure 10b. Resins increased and grooves decreased on the fracture surfaces with the increase of La^{3+} concentration, as seen in Figure 10c,d. These residual resins on the fibers' surfaces were attributed in the improved adhesion between fibers and the resin matrix, when fibers were stretched from the resin matrix under the stress. When La^{3+} concentration was up to 0.5 wt.%, the gaps between fibers were filled with the resins in Figure 10d. BFs and the resin matrix adhered so tightly that external load was delivered to the fibers from the matrix, and the fibers mainly tolerated the breaking stress. It exhibited the obviously improved mechanical properties of BF/ERCs in the better reinforcing effect.

When La^{3+} concentration exceeded 0.5 wt.%, the decrease in resins on the fiber surfaces with increasing La^{3+} concentration led to the reappeared grooves on the resin matrix, when the smooth fibers pulled out, as seen in Figure 10e,f. It demonstrated that the interfacial strength between the fibers and the resin matrix reduced, and the mechanical properties of composites correspondingly decreased.

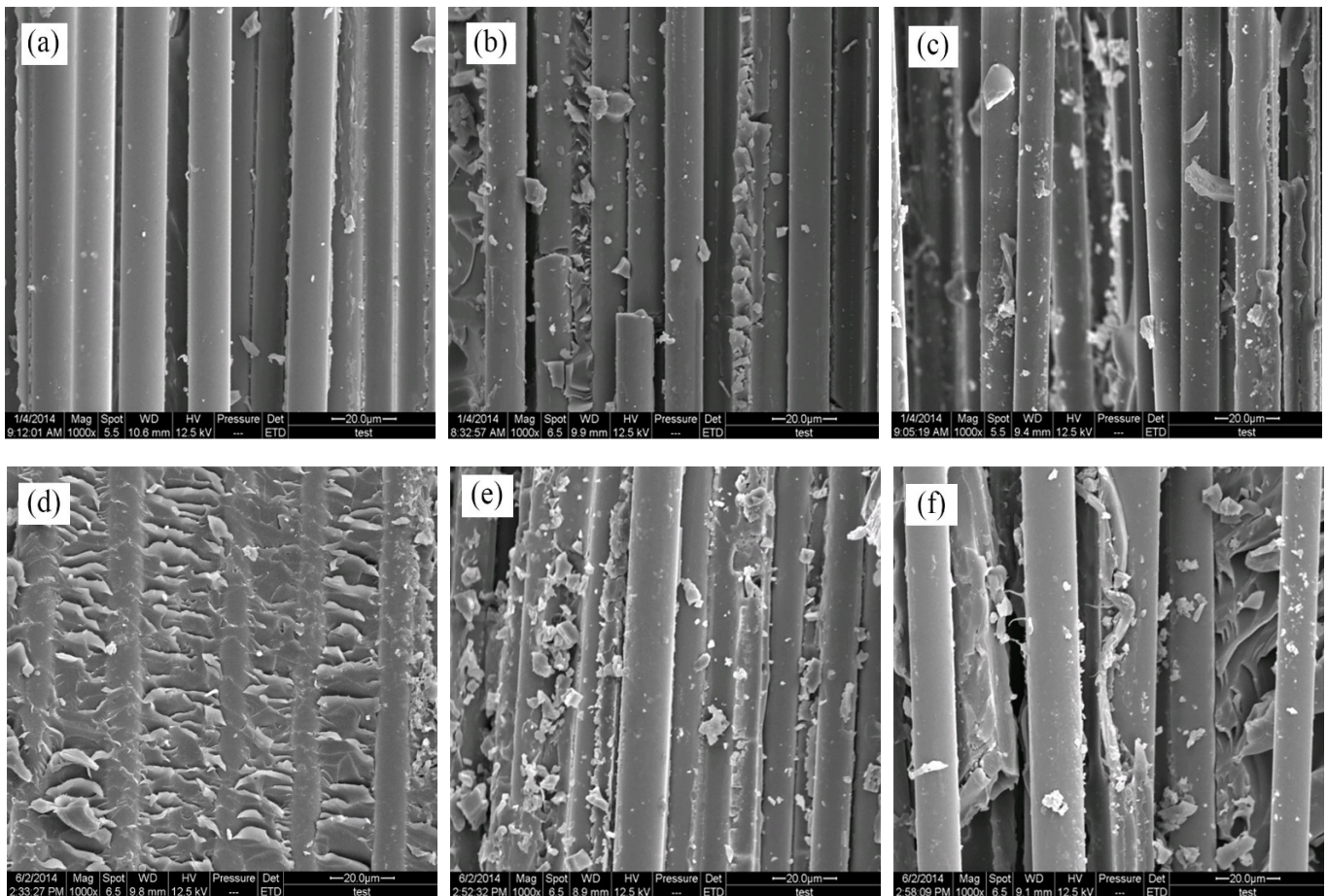


Figure 10. SEM images of fracture surfaces of BF/ERCs: (a) untreated; (b) treated with modification solution containing La^{3+} 0.1 wt.%; (c) treated with modification solution containing La^{3+} 0.3 wt.%; (d) treated with modification solution containing La^{3+} 0.5 wt.%; (e) treated with modification solution containing La^{3+} 0.7 wt.%; (f) treated with modification solution containing La^{3+} 0.9 wt.%.

The monomolecular layer theory can be supplemented to analyze the effect of element La concentration on the tensile performances of BF/ERCs with the model shown in Figure 11. At low concentrations, few La^{3+} were absorbed onto the BF's surfaces. As shown in Figure 11a, the arrangement of La atoms on BF's surfaces was discontinuous with a lot of voids, resulting in the failure of BF/ERCs occurring firstly on the location without La atoms under external load. Thus, the discontinuous interface between BF's and the epoxy resin is insufficient to improve the mechanical performance of BF/ERCs obviously. When La element increased to the best concentration, 0.5 wt.%, the uniform and compact monomolecular layer on the BF's surfaces exhibits high adhesive strength between BF's and the matrix, as shown in Figure 11b. The mechanical performances of BF/ERCs reached to the highest value, including the tensile strength, the bending strength, and ILSS.

When La^{3+} concentration exceeded 0.5 wt.%, excessive La atoms were assembled on the BF's surfaces to form multimolecular layer, as shown in Figure 12. Under external load, failure of BF/ERCs firstly occurred on the interlayer of La atoms interlinked by weak Van der Waals force, resulting in the decreased performance of BF/ERCs.

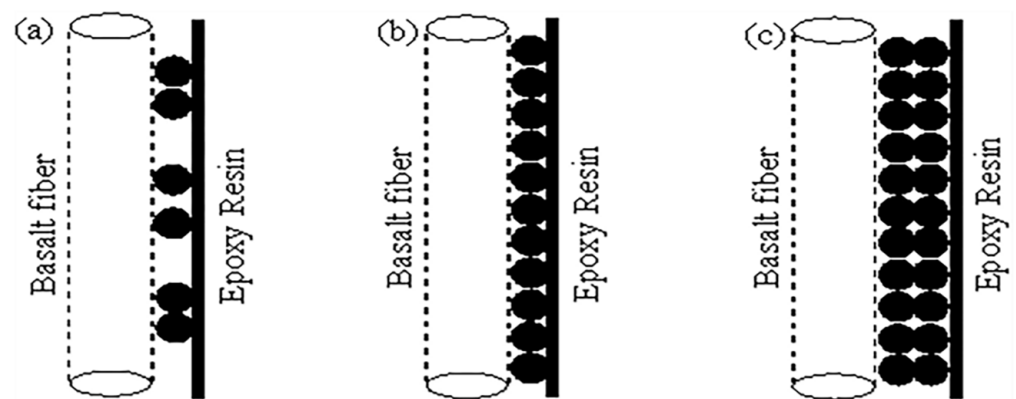


Figure 11. Model of monomolecular layer theory. (a) the model with less La^{3+} ; (b) the model with enough La^{3+} ; (c) the model with excess La^{3+} .

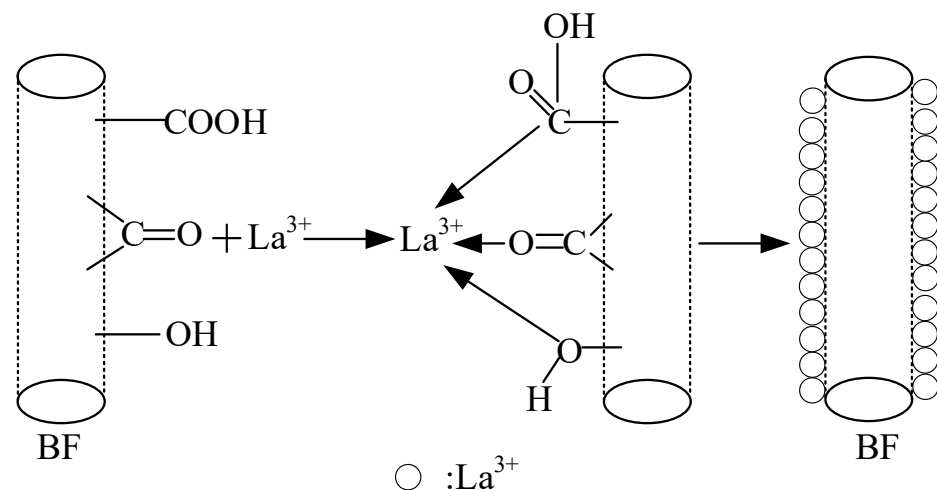


Figure 12. La^{3+} attached onto BFs surfaces.

4. Discussion

4.1. Analysis about Modification Mechanism of La^{3+}

In Figures 1–5, the analysis based on the FT-IR spectra and the XPS results of BFs shows that, compared to untreated BFs, active oxygen-containing functional groups on the fiber surfaces increased, once BFs is treated with the rare earth modification solution. That was ascribed to the mechanism of La element in the modification solution as follows.

The rare earth elements with 4f electronic shell have good chemical activity. Once polarized, they have strong affinity to the nonmetal elements and turn into active elements in alcohol solution with the typical nonmetal elements such as C, H, O and N [26–28]. Consequently, with the results in Section 3.2.2., the coordination bonds between La ions and nonmetal elements are formed and La elements are attached onto the fiber surfaces, as shown in Figure 12.

The coordination number of La element changes from 3 to 12, while the majority level remains 8. In this study, the rare earth modification solution was the alcohol solution with a variety of organic compounds, such as urea and citric acid, as shown in Figure 13a. As the active chemical cores, La ions attached on the BFs surfaces were combined with a lot of active organic groups in the solution to generate the multicomponent complex [26–28], shown in Figure 13b. With the active organic groups absorbed onto the fiber surfaces to form the macromolecular membrane, the chemical activity on the fiber surfaces could be improved obviously, as shown in Figure 13c. As seen in Figure 6, the La ions can also be

embedded in the defect points on the BFs surfaces to generate more active chemical cores, and hence the chemical activity of the fiber surfaces can be further improved.

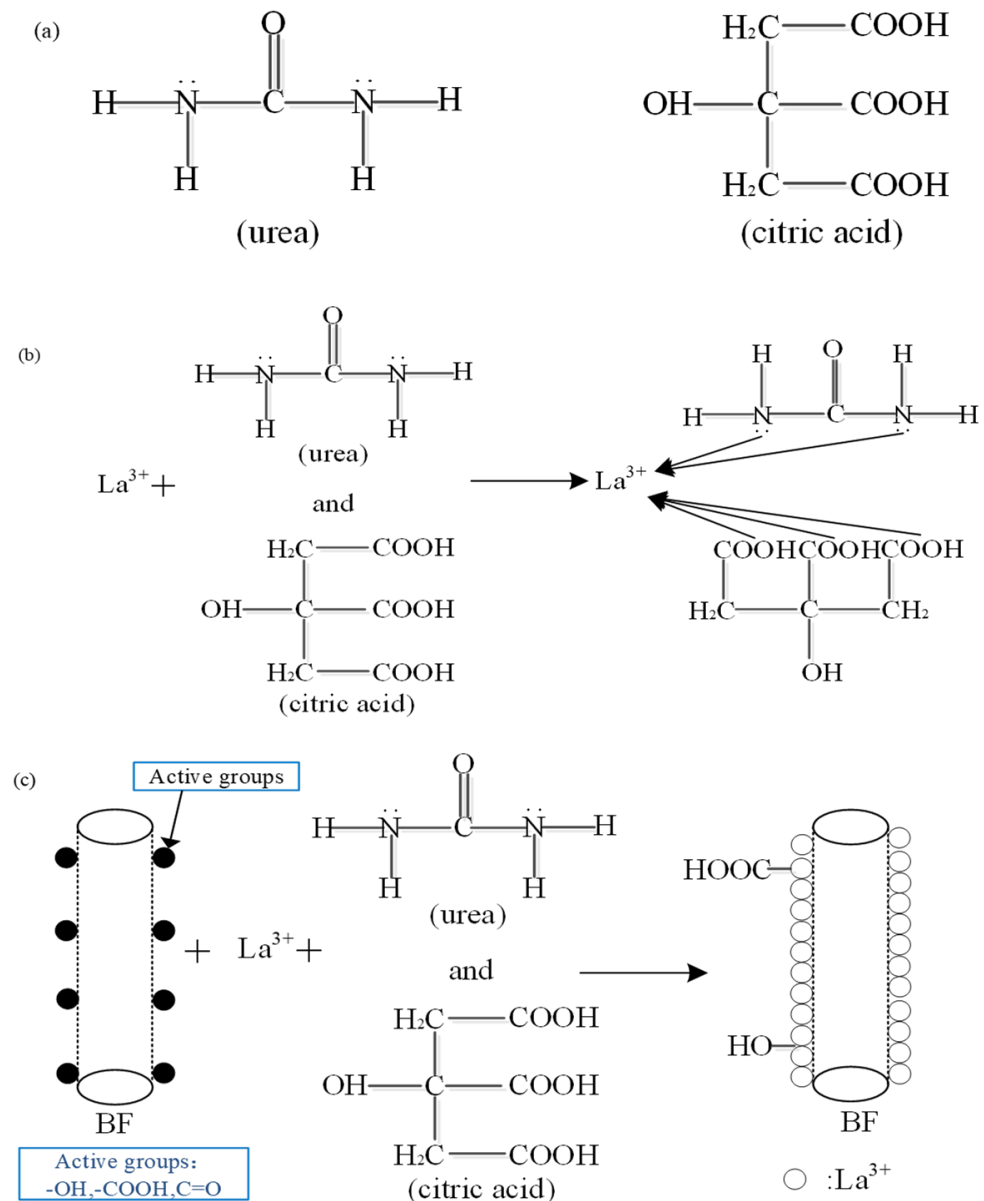


Figure 13. The chemical reaction mechanism of the La^{3+} modification solution: (a) the molecular formula of urea and citric acid in the modification solution; (b) the chemical combination between La^{3+} and the active groups in the modification solution; (c) the chemical combination between the BFs and the modification to introduce the more active groups.

However, the abundant active groups introduced by the excess La^{3+} were aggregated on the fibers' surfaces to be supersaturated, resulting in the break of the macromolecular membrane and loss of active groups, as shown in Figure 4e,f. Meanwhile, with the excess La^{3+} , the generated Si-OH between SiO_2 of the fibers' surface and the modification solution under hydrolytic action restrain the further hydrolytic action of SiO_2 , leading to the decrease of Si-OH and Si-O-Si in Figure 4e,f, which further reduced the surface activity of fibers. Thus, the La^{3+} concentration of 0.5% was the most suitable.

4.2. Analysis of Enhancement Mechanism of BFs/ECR's Mechanical Property Modified with La^{3+}

In the process of the resin matrix synthesis, the following crosslinking reaction of epoxy resin with ali-phatic polyamine curing agent took place and generated two oxhydryl groups, as shown in Figure 14.

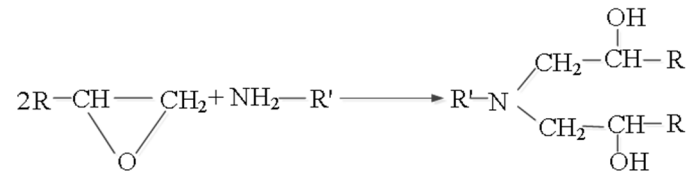


Figure 14. The crosslinking reaction of epoxy resin with aliphatic polyamine curing agent.

Based on the FT-IR spectra and the XPS results of BFs, the active functional groups increased on the surface of BFs treated with the rare earth modification solution. With the oxhydryl generated in the above crosslinking reaction, the active functional groups took part in the dehydration condensation reaction, when BFs were in sufficient contact with epoxy resin. The bonding of BFs and epoxy resin was based on the chemical bonds, such as the ester group and the ether bond, so that the bonding force improved significantly, as shown in Figure 15a. Thus, when La^{3+} concentration was 0.5 wt.%, the absorbed active groups reached to the maximum and the bonding force was correspondingly highest, as well as the tensile strength, the bending strength, and ILSS.

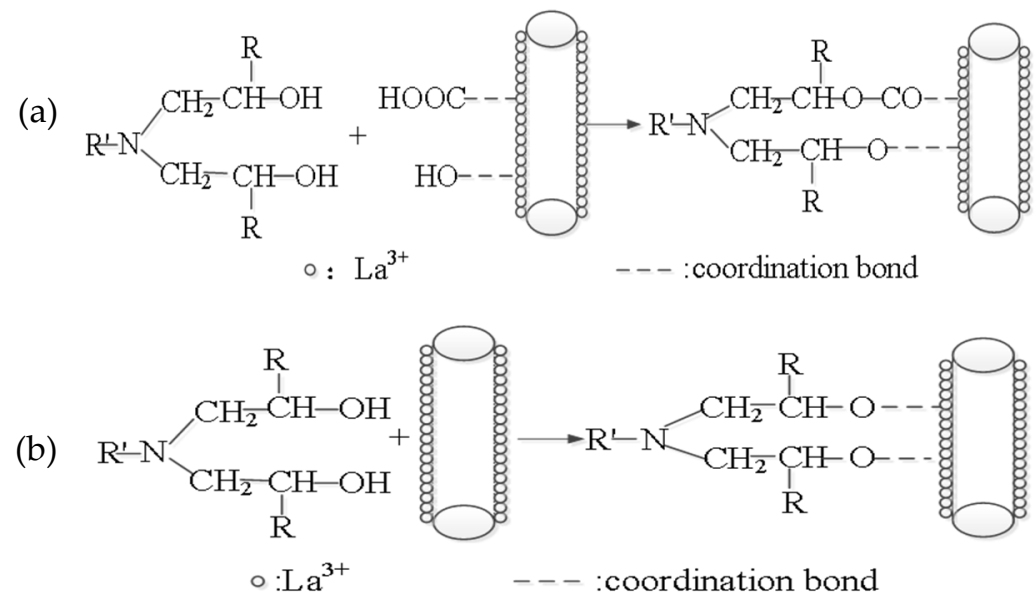


Figure 15. Effect of La^{3+} on the interface of BFs and epoxy resin. (a) the chemical reaction between the absorbed active groups and the epoxy resin containing curing agent; (b) the coordination reaction between La^{3+} and the epoxy resin containing curing agent.

However, parts of La ions, which were absorbed on the modified BFs surfaces, did not take part in the coordination bond with active groups. When the modified BFs were put into the epoxy resin, these La ions can be combined with oxhydryl generated in the above crosslinking reaction, because of the typical chemical activities and the variable coordination number of La^{3+} . As shown in Figure 15b, under the effect of the formed coordination bond, the adhesion strength between BFs and epoxy matrix was further improved, as well as the mechanical performances of BF/ERCs.

5. Conclusions

In this research, the modification of basalt fibers with the modification solution of different La^{3+} concentrations was carried out. Moreover, the effect of modification with different La^{3+} concentrations and the mechanical properties for basalt fiber/epoxy resin composites modified with La^{3+} were evaluated.

The study about the chemical composition, the functional groups and the morphology of untreated and treated BFs' surface with the rare earth modification solution using several analytical techniques (FTIR, XPS, and SEM), confirmed that La element in the rare earth modification solution could link active oxygen-containing functional groups to the BFs surfaces to improve the roughness and the activity of the fiber surfaces. When the La^{3+} concentration in the rare earth modification solution was 0.5 wt.%, the activity of BFs' surface reached the strongest with the most introduced active groups. It is also determined that the mechanical performances of BF/ERCs, including the tensile strength, the bending strength and ILSS, could be significantly enhanced by the modified BFs due to the formed chemical reaction between resin matrix and the more active groups introduced by La^{3+} . With the La^{3+} concentration in the rare earth modification solution reaching 0.5 wt.%, the bonding between the resin matrix and BFs is demonstrated to be the best and the tensile strength, the bending strength and ILSS were up to 458.7, 556.7 and 16.77 Mpa, and improved by 56.22%, 103.32% and 88% compared with those of the unmodified ones, respectively.

In addition, the modification mechanism of La^{3+} and enhancement mechanism of BFs/ECR's mechanical property modified with La^{3+} were stated with the strong affinity of La to the nonmetal elements, indicating that the modification of BFs with La^{3+} was effective and the mechanical property of the prepared BFs/ECR composites was excellent.

Author Contributions: Conceptualization, C.L.; methodology, C.L.; software, H.W.; validation, C.L., X.H. and Y.F.; formal analysis, C.L.; investigation, C.L., H.W. and Y.S.; resources, C.L.; data curation, Y.S.; writing—original draft preparation, C.L. and H.W.; writing—review and editing, C.L., H.W. and X.Z.; visualization, H.W. and X.Z.; supervision, C.L.; project administration, C.L.; funding acquisition, C.L. All authors have read and agreed to the published version of the manuscript.

Funding: The research was funded by Science Foundation of the National Key Laboratory of Science and Technology on Advanced Composites in Special Environment (Grand No. JCKYS2019603C006).

Institutional Review Board Statement: Not applicable.

Informed Consent Statement: Not applicable.

Data Availability Statement: The data presented in this study are available on request from the corresponding author. The data are not publicly available as the data also form part of an ongoing study.

Conflicts of Interest: The authors declare no conflict of interest.

References

1. Wei, B.; Song, S.; Cao, H. Strengthening of basalt fibers with nano- SiO_2 -epoxy composite coating. *Mater. Des.* **2011**, *32*, 4180–4186. [[CrossRef](#)]
2. Dhand, V.; Mittal, G.; Rhee, K.Y.; Park, S.J.; Hui, D. A short review on basalt fiber reinforced polymer composites. *Compos. Part B Eng.* **2015**, *73*, 166–180. [[CrossRef](#)]
3. Manikandan, V.; Jappes, J.; Kumar, S.; Amuthakkannan, P. Investigation of the effect of surface modifications on the mechanical properties of basalt fibre reinforced polymer composites. *Compos. Part B Eng.* **2012**, *43*, 812–818. [[CrossRef](#)]
4. Lopresto, V.; Leone, C.; De Iorio, I. Mechanical characterisation of basalt fibre reinforced plastic. *Compos. Part B Eng.* **2011**, *42*, 717–723. [[CrossRef](#)]
5. Colombo, C.; Vergani, L.; Burman, M. Static and fatigue characterisation of new basalt fibre reinforced composites. *Compos. Struct.* **2012**, *94*, 1165–1174. [[CrossRef](#)]
6. Wei, B.; Cao, H.; Song, S. Surface modification and characterization of basalt fibers with hybrid sizings. *Compos. Part A* **2011**, *42*, 22–29. [[CrossRef](#)]
7. Scalici, T.; Valenza, A.; Di Bella, G.; Fiore, V. A review on basalt fibre and its composites. *Compos. Part B Eng.* **2015**, *74*, 74–94.
8. Arvin, A.C.; Bakis, C.E. Optimal design of press-fitted filament wound composite flywheel rotors. *Compos. Struct.* **2006**, *72*, 47–57. [[CrossRef](#)]

9. Rashkovan, I.A.; Korabel'nikov, Y.G. The effect of fiber surface treatment on its strength and adhesion to the matrix. *Compos. Sci. Technol.* **1997**, *57*, 1017–1022. [[CrossRef](#)]
10. Lee, S.O.; Rhee, K.Y.; Park, S.J. Influence of chemical surface treatment of basalt fibers on interlaminar shear strength and fracture toughness of epoxy-based composites. *J. Ind. Eng. Chem.* **2015**, *32*, 153–156. [[CrossRef](#)]
11. Kim, M.T.; Kim, M.H.; Rhee, K.Y.; Park, S.J. Study on an oxygen plasma treatment of a basalt fiber and its effect on the interlaminar fracture property of basalt/epoxy woven composites. *Compos. Part B Eng.* **2011**, *42*, 499–504. [[CrossRef](#)]
12. Schneck, T.K.; Brück, B.; Schulz, M.; Spörl, J.; Hermanutz, F.; Clauß, B.; Mueller, W.M.; Heidenreich, B.; Koch, D.; Horn, S.J.; et al. Carbon fiber surface modification for tailored fiber-matrix adhesion in the manufacture of C/C-SiC composites. *Compos. Part A Appl. Sci. Manuf.* **2019**, *120*, 64–72. [[CrossRef](#)]
13. Jiang, T.; Li, Z.; Xiao, P.; Liu, J.; Liu, P.; Yu, S.; Xiao, T.; Liu, L.; Technology, C. Effect of different chemical treatments on hydroxyapatite formation of carbon fibers reinforced carbon and SiC dual matrices composites. *Surf. Coat. Technol.* **2019**, *357*, 153–160. [[CrossRef](#)]
14. Dighton, C.; Rezai, A.; Ogin, S.L.; Watts, J.F. Atmospheric plasma treatment of CFRP composites to enhance structural bonding investigated using surface analytical techniques. *Int. J. Adhes. Adhes.* **2019**, *91*, 142–149. [[CrossRef](#)]
15. Cho, B.G.; Hwang, S.H.; Park, M.; Park, J.K.; Park, Y.B.; Chae, H.G.J.C. The effects of plasma surface treatment on the mechanical properties of polycarbonate/carbon nanotube/carbon fiber composites. *Compos. Part B Eng.* **2019**, *160*, 436–445. [[CrossRef](#)]
16. Cech, V.; Knob, A.; Lasota, T.; Lukes, J.; Drzal, L.T.J.P.C. Surface modification of glass fibers by oxidized plasma coatings to improve interfacial shear strength in GF/polyester composites. *Polym. Compos.* **2019**, *40*, E186–E193. [[CrossRef](#)]
17. Arslan, C.; Dogan, M.J. The effects of fiber silane modification on the mechanical performance of chopped basalt fiber/ABS composites. *J. Thermoplast. Compos. Mater.* **2019**, *33*, 089270571982951. [[CrossRef](#)]
18. Latif, R.; Wakeel, S.; Khan, N.Z.; Siddiquee, A.N.; Verma, S.L.; Khan, Z.A. Surface treatments of plant fibers and their effects on mechanical properties of fiber-reinforced composites: A review. *J. Reinf. Plast. Compos.* **2019**, *38*, 15–30. [[CrossRef](#)]
19. Iorio, M.; Santarelli, M.L.; González-Gaitano, G.; González-Benito, J. Surface modification and characterization of basalt fibers as potential reinforcement of concretes. *Appl. Surf. Sci.* **2018**, *427*, 1248–1256. [[CrossRef](#)]
20. Xu, Z.; Wu, X.; Ying, S.; Jiao, Y.; Li, J.; Li, C.; Lu, L. Surface modification of carbon fiber by redox-induced graft polymerization of acrylic acid. *J. Appl. Polym. Ence.* **2010**, *108*, 1887–1892. [[CrossRef](#)]
21. Jiang, Z.X.; Liu, L.; Huang, Y.D.; Ren, H. Influence of coupling agent chain lengths on interfacial performances of carbon fiber and polyarylacetylene resin composites. *Surf. Interface Anal.* **2010**, *41*, 624–631. [[CrossRef](#)]
22. Li, K.Z.; Wang, C.; Li, H.J.; Li, X.T.; Ouyang, H.B.; Jian, W. Effect of chemical vapor deposition treatment of carbon fibers on the reflectivity of carbon fiber-reinforced cement-based composites. *Compos. Sci. Technol.* **2008**, *68*, 1105–1114. [[CrossRef](#)]
23. Hung, K.B.; Li, J.; Fan, Q.; Chen, Z.H. The enhancement of carbon fiber modified with electropolymer coating to the mechanical properties of epoxy resin composites. *Compos. Part A Appl. Sci. Manuf.* **2008**, *39*, 1133–1140. [[CrossRef](#)]
24. Jain, N.; Singh, V.K.; Chauhan, S. Review on effect of chemical, thermal, additive treatment on mechanical properties of basalt fiber and their composites. *J. Mech. Behav. Mater.* **2018**, *26*, 205–211. [[CrossRef](#)]
25. Ricciardi, M.R.; Papa, I.; Coppola, G.; Lopresto, V.; Sansone, L.; Antonucci, V. Effect of plasma treatment on the impact behavior of epoxy/basalt fiber-reinforced composites: A preliminary study. *Polymers* **2021**, *13*, 1293. [[CrossRef](#)] [[PubMed](#)]
26. Ju, W.; Cheng, X. Effect of rare earth modifier treatment on interlaminar shear strength of aramid/epoxy composites. *Rare Met. Mater. Eng.* **2005**, *34*, 1917–1920.
27. Bao, D.; Cheng, X.H. The effect of rare earth treatment on tensile properties of carbon fiber reinforced polytetrafluoroethylene composites. *J. Shanghai Jiaotong Univ.* **2006**, *40*, 914–917.
28. Wu, J.; Cheng, X.H. Effect of rare earth treatment on tensile properties of F-12 fiber reinforced epoxy composites. *J. Shanghai Jiaotong Univ.* **2005**, *39*, 1795–1798.
29. Jin, T.; Shen, S.; Jing, L.I.; Weina, L.I.M.R. Feasibility study of a new method of basalt fiber surface treatment-acid etching treatment. *Mater. Rev.* **2014**, *12*, 116–118.